EPR spin trapping Evidence of Radical Intermediates in the Photo-reduction of Bicarbonate/CO_2 in TiO_2 Aqueous Suspensions

Alessandra Molinari,[1]* Luca Samiolo,[2] Rossano Amadelli, [2]*

[1]Dipartimento di Scienze Chimiche e Farmaceutiche, University of Ferrara, via Fossato di Mortara 17, I-44121 Ferrara, Italy. E-mail: alessandra.molinari@unife.it Tel. +39 0532 455378

[2]CNR-ISOF U.O.S. of Ferrara, c/o Department of Chemistry, University of Ferrara, via Fossato di Mortara 17, I-44121 Ferrara, Italy. E-mail: amr@unife.it Tel. +39 0532 455161. lucasamiolo@gmail.com

Abstract

Using the EPR spin trapping technique, we prove that simultaneous reactions taking place in illuminated suspensions of TiO_2 in aqueous carbonate solutions (pH ≈ 7). Adsorbed HCO_3^- is reduced to formate as directly made evident by the detection of formate radicals ($^\bullet CO_2^-$). Additionally, the amount of $OH^\bullet$ radicals from the photo-oxidation of water shows a linear dependence on the concentration of bicarbonate, indicating that electron scavenging by HCO_3^- increases the lifetime of holes. In a weakly alkaline medium, photo-oxidation of HCO_3^-/CO_3^{2-} to $^\bullet CO_3^-$ interferes with the oxidation of water. A comparative analysis of different TiO_2 samples shows that formation of ($^\bullet CO_2^-$) is influenced by factors related to the nature of the surface, once expected surface area effects are accounted for. Modification of TiO_2 surface with noble metal nanoparticles does not have unequivocal benefits: the overall activity improves with Pd and Rh but not with Ru which favours HCO_3^- photo-oxidation even at pH =7.

In general, identification of radical intermediates of oxidation and reduction reactions can provide useful mechanistic information that may be used in the development of photocatalytic systems for the reduction of CO_2 also stored in the form of carbonates.

Introduction

Carbon dioxide is the most abundant form of oxidized carbon occurring in nature. Its conversion to useful chemicals has been the aim of intense research over several decades and is presently experiencing an important surge of interest as concern is growing over the threat of greenhouse effects. [1-3] Unfortunately, it is a prominent result of both experimental [4-7] and theoretical [8] studies that the reductive conversion of CO_2 is a difficult, challenging process. It is currently understood that $^{\bullet}CO_2^-$ is the key surface intermediate in both electro-catalytic and photocatalytic reduction on semiconductors

$$CO_2 + e^- \rightarrow {}^{\bullet}CO_2^- \qquad (1)$$

which can subsequently undergo multielectron reduction to formate, CO and further to methanol and methane.

The redox potential of reaction (1) is -1.9 V vs. NHE, and understandably electrochemical reduction is advantageous due to the possibility to span a large interval of potentials. Results of electrochemical studies focusing on application have already appeared in the literature [9,10] although the competing evolution of hydrogen can be a limitation still requiring efforts towards an optimized choice of the metal electrode. [6] Conversely, the redox potential is far too negative compared to the energy of photo-generated electrons on most semiconductors [5] in aqueous media; in consequence, the occurrence of reaction (1) appears thermodynamically impossible in the photocatalytic approach.

Photocatalysis, on the other hand, has the important advantage of sustainability in that light is used as a continuous source of renewable energy for reactions to occur on stable and environmentally benign semiconductors such as TiO_2. It stands to reason, then, that research in this field continues to be

very active [11-13], with particular attention being paid to activation of the rather inert CO_2 molecule. Indeed this is the most important step in any reaction of CO_2 basically involving the transformation of its linear structure into a more reactive bent form, i.e., in a state in which the LUMO is lowered enough to facilitate electron transfer.[7] Conditions become favorable when CO_2 is coordinated to active centers of homogenous phase molecular catalysts or when it is adsorbed on surfaces. [14] In this regard, earlier [13,15] and recent[16-19] studies have underlined the advantages of CO_2 conversion to carbonate/bicarbonate which, upon adsorption, may undergo an easier reduction. In an interesting recent paper it has been showed that in CO_2-saturated bicarbonate solutions (pH 6.8), bicarbonate undergoes electrochemical reduction first to produce formate and at higher applied potentials, CO_2 is reduced to CO.[19]

Reduction of CO_2 is a multielectron process that leads to formation of various products via different pathways that depend on the characteristics of the catalyst employed , [11] among other factors. Basic questions that have been posed concern the dynamics of electron transfer and the identification of the active surface sites. [7] Then, the analysis of reaction mechanisms has a fundamental importance since understanding of the basic reaction steps is a critical aspect in the design of selective and efficient systems. In particular one needs information about the initial steps of the CO_2 reductive activation which has been given less attention in comparison, for example, with processes such as the oxidation of water or alcohols. In this context, a recent electron paramagnetic resonance (EPR) study by Dimitrijevic et al. [20] is to be signaled as an important contribution. The EPR technique offers indeed a potent tool for the detection of short-lived radical species. [21-24]

These considerations are the motivation that led us to undertake the investigations described in the present paper. Specifically, we used the EPR spin-trapping technique to analyse directly the formation and the role of radical intermediates in illuminated deaerated TiO_2 aqueous suspensions containing carbonates, under photocatalytic conditions in which water oxidation and reduction processes are required to occur simultaneously.

Results and Discussion

Photocatalysis on semiconductors, such as titanium dioxide, is based on the photo-generation of charges: positive holes in the valence band (h_{vb}^+) of the oxide and electrons in its conduction band (e_{cb}^-) according to Eq. 2.

$$TiO_2 + h\nu \longrightarrow h_{vb}^+ + e_{cb}^- \qquad (2)$$

In order to achieve an efficient photocatalytic process, holes and electrons have to be quickly transferred to donor and acceptor species. Since oxidation and reduction processes occur on the same photoexcited particle, at steady state conditions the two rates must be equal on the basis of a charge balance requirement. In principle one can, for example, gain information about the reduction reaction by following the time course of the oxidation process, which indeed has been verified in some instances. [25] For the case of transient measurements, however, it might be an optimistic hypothesis since electrons or holes can accumulate during short time experiments instead of being transferred to acceptor or donor species, respectively. In the following, we will explore factors that influence the reduction of bicarbonate and the oxidation of water, which are closely connected processes taking place on different sites of the same photocatalyst particle.

Effect of $NaHCO_3$ on the formation $OH^\bullet$ radicals

In our deaerated aqueous $NaHCO_3/CO_2$ system, water oxidation by holes occurs with formation of $OH^\bullet$ radicals (Eq. 3) and since direct reduction of bicarbonate is emphasized in several literature reports, [13-20] one can assume in a first approach that adsorbed HCO_3^- is the electron scavenger (Eq. 4).

Monitoring of hydroxyl radicals by EPR spin trapping technique gives at least an indirect indication about reduction of carbonates.

$$H_2O + h^+ \longrightarrow OH^\bullet + H^+ \quad (3)$$

$$HCO_3^- + 2e^- + 2H^+ \longrightarrow HCO_2^- + H_2O \quad (4)$$

The reported thermodynamic potential of the process described by Eq. 4 is –0.52 V [13] and the mechanism seemingly involves a concerted proton and electron transfer.[20] Regarding reaction 3, it is noteworthy that under short time illumination, the species trapping holes may be actually surface OH groups.

In our study we use α-phenyl N-*tert*-butyl nitrone (pbn) as a spin trap. Its reaction with $OH^\bullet$ radicals leads to a paramagnetic adduct $[pbn\text{-}OH]^\bullet$ that can be identified by both the hyperfine structure and the coupling constants values.[26] In the literature, 5,5-dimethyl pyrroline *N*-oxide (DMPO) is often used as a spin trap because the signal of $[DMPO\text{-}OH]^\bullet$ adduct has peculiar characteristics that facilitate the identification of the trapped radical. [23, 24, 26] However, we decided that DMPO is not reliable in our study because its adducts with $^\bullet CO_2^-$ and $^\bullet CO_3^-$ radicals intermediates are not stable; after a fast rearrangement they actually evolve to $[DMPO\text{-}OH]^\bullet$, giving misleading information about the mechanism of radicals formation in the photocatalytic process.[27]

When deaerated aqueous suspensions (pH ≈ 7) of TiO_2-P25 containing pbn are illuminated, one observes EPR spectra consisting of a triplet of doublets (Fig.1 curve 1) with coupling constants a_N= 15.4 G and a_H= 2.8 G. In agreement with literature,[26] this signal is attributed to the paramagnetic adduct $[pbn\text{-}OH]^\bullet$, confirming the formation of $OH^\bullet$ radicals (Eq. 3). An analogous experiment was carried out starting from deaerated suspensions containing $NaHCO_3$ (0.01 M, initial pH was 8.8,

brought to pH 7÷7.5 by bubbling of CO_2). The spectra recorded upon illumination reveal again the [pbn-OH]$^{\bullet}$ adduct (Fig. 1 curve 2) and, notably, signal intensities are greater when bicarbonate is present, for the same pH conditions. Although the trapping process in not quantitative, the amount of trapped radicals can be considered constant if an excess of spin trap is used.[28] On this basis, one can compare spectra obtained under identical experimental conditions and safely assume a proportionality between the signal intensity and the concentration of photo-generated radicals.

In addition, another signal is observed in Fig. 1 (marked *) consisting of a quartet with $a_N = a_H =$ 14.2 G. In accordance with literature,[29] this quartet is ascribed to trapped $^{\bullet}CO_3^-$ radicals which can be formed from reaction between bicarbonate ions and $OH^{\bullet}$ radicals (Eq. 5):

$$HCO_3^- + OH^{\bullet} \longrightarrow {}^{\bullet}CO_3^- + H_2O \quad (5)$$

FIGURE 1

Photo-oxidation of carbonate/bicarbonate to $^{\bullet}CO_3^-$ radicals has been observed before [20] in the EPR spectra, but at 4.5 K.

Reduction of HCO_3^-/CO_2 should be favored by a pH increase since the flat band potential becomes more negative according to:

$$E_{fb} = E_{fb}\,(pH=0) - 0.06\ pH \quad (6)$$

However, as pH is increased, photo-oxidation of HCO_3^-/CO_3^{2-} (Eq. 5) can compete with its reduction (Eq. 4) as demonstrated by Sayama and Arakawa [30] who have also emphasized the role of $^{\bullet}CO_3^-$ radical intermediates in promoting O_2 evolution on TiO_2 at pH > 10 and described a reaction mechanism of $^{\bullet}CO_3^-$ formation from carbonate oxidation in an alkaline medium.

Our results showed that in our experimental conditions (pH < 8), the intensity of the signal due to the [pbn-CO_3^-]$^\bullet$ adduct is at least 5-fold less than that at pH = 10 for the same illumination time (2 min). Importantly, no intensity increase with irradiation time was observed in neutral solutions, indicating that the reaction between HCO_3^- and OH$^\bullet$ radicals (Eq. 5) is here a minor pathway that does not proceed to any appreciable degree and does not interfere with trapping of other radicals. We also point out that occurrence of reaction (5) to any significant extent would lead to an important decrease of the [pbn-OH]$^\bullet$ signal intensity that was not observed at pH < 8. On the contrary, Fig. 2 shows that the [pbn-OH]$^\bullet$ intensity increases linearly as the $NaHCO_3$ concentration is increased.

FIGURE 2

Since the pH was kept at 7÷7.5 in these experiments, HCO_3^- constitutes more than 80% of all the inorganic carbon forms in the solution (CO_2/ HCO_3^-/ CO_3^{2-}). The ratio between the species in the equilibrium

$$CO_2 + H_2O \rightleftharpoons HCO_3^- + H^+ \qquad (7)$$

will remain constant in the dark while, under illumination, it might shift to right side if HCO_3^- is photo-reduced. In turn, consumption of electrons in this process will increase the lifetime of holes and favor the oxidation of water involving OH radical intermediates, as seen in Fig. 2.

We have performed additional experiments in which either the concentration of $NaHCO_3$ or pH was changed. The intensities of the [pbn-OH]$^\bullet$ adduct that is formed upon illumination of TiO_2-P25 in these media are reported in Figure 3. Comparison of entries 1-3 confirms that an increase in the concentration of $NaHCO_3$ results in a corresponding increase of the [pbn-OH]$^\bullet$ intensity. Sample 4

refers to a system obtained by bubbling CO_2 through a bicarbonate solution until a final pH of 5.5. At this pH value about 70% of all the carbon forms is CO_2/H_2CO_3 and one notes a substantial increase of $OH^{\bullet}$ radicals as revealed by the greater intensity of the $[pbn\text{-}OH]^{\bullet}$ adduct.

To a first analysis, this result would indicate that carbon dioxide is a very good electron acceptor, which would decrease recombination and in consequence enhance water oxidation by holes. However, we noted that the recorded $[pbn\text{-}OH]^{\bullet}$ intensity for illuminated TiO_2 aqueous suspensions saturated with CO_2 until pH 4.2 (entry 5) is comparable to that obtained in dearated water (entry 1) and lower than that obtained at a pH of 5.5 (entry 4). At pH ≈ 4 there are no bicarbonate anions in equilibrium with carbon dioxide and this leads one to conclude that electron capture by dissolved CO_2 is inefficient, in accordance with the poor interaction of the unactivated molecule with TiO_2. The possible explanation for the higher amount of $OH^{\bullet}$ radicals measured at pH = 5.5 (sample 4) is that this pH is lower than the point of zero charge (PZC ~ 7 for P-25) and the TiO_2 surface charge is positive. This condition is expected to enhance adsorption of the bicarbonate anion, as shown in Equation 8,

$$TiOH_2^+ + HCO_3^- \rightleftharpoons TiOCO_2^- + H_2O + H^+ \qquad (8)$$

FIGURE 3

and, in fact, adsorption is evident in a comparison of cyclic voltammetry curves (ESI Fig. 1) recorded in $NaHCO_3$ at pH 7 and 5.5. In the latter case one notes new cathodic and anodic peaks that reflect significant changes in the band-gap states.

In order to buttress the conclusions of EPR results, we used the hydroxylation of coumarin as an independent method to verify the effect of bicarbonate on the formation of OH radicals. [31, 32]

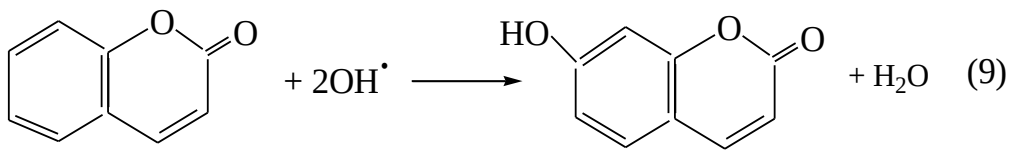

(9)

Formation of 7-hydroxycoumarin (7-HC) (Eq. 9) can be followed by emission spectroscopy as it gives an intense luminescence upon UV light excitation. The results displayed in Fig. 4 clearly show that the intensity emission spectra depends on $NaHCO_3$ (curves 1-3) and, moreover, measurements at different concentrations showed that the dependence is linear, confirming the EPR data of Fig. 2. The emission intensity of 7-HC formed at pH ≈ 4 is significantly lower than that at pH 5.5 (ESI, Fig. 2) and, in agreement with EPR results (see above, entry 5 of Fig. 3), $OH^{\bullet}$ radicals formation is a comparatively less efficient process when CO_2/H_2CO_3 are the dissolved species.

Additionally, as pH increase from 7 to 10 the fluorescence intensity increases in the absence of bicarbonate and decreases in its presence (ESI 3). The lower OH radical formation caused by the carbonate is in accordance with reaction 5.

FIGURE 4

Evidence of formate production through detection of $^{\bullet}CO_2^-$ radicals.

The results reported above seemingly suggest that bicarbonate anions can act as the electron acceptors thus improving both charge separation and the efficiency of water photo-oxidation. This conclusion is consistent with experimental facts but it is based on indirect evidence of the photo-reduction of HCO_3^-. In the following we will give a proof of the occurrence of bicarbonate reduction to formate by showing that formation of $^{\bullet}CO_2^-$ radicals that can be directly revealed by EPR spin

trapping. Interestingly though, these radicals were not detected in a previous work in which DMPO was used as the spin trap.[20]

Figure 5 displays the effect of illumination time on the EPR spectra for a TiO_2-P25 suspension in a $NaHCO_3$ solution. In the short time scale (< 60 s, curve 1) the only observed spectrum corresponds to the [pbn-OH]$^\bullet$ adduct (cfr. Fig. 1) while a new, well defined triplet of doublets, with hyperfine coupling constants of a_N = 15.5 G and a_H = 4.7 G, appears on prolonging irradiation (3 min). These last parameters correspond to the trapping of formate radicals $^\bullet CO_2^-$ by pbn [26] and, interestingly, its detection might imply reduction of bicarbonate (Eq. 4).

FIGURE 5

One possibility would be that formate is accumulated in sufficient amount to give $^\bullet CO_2^-$ by reaction with OH$^\bullet$ radicals ($k = 3.5 \times 10^9\ M^{-1}\ s^{-1}$) according to Eq. 10:

$$OH^\bullet + HCO_2^- \rightarrow H_2O + {}^\bullet CO_2^- \qquad (10)$$

But actually, since experiments refer to initial phenomena, occurring at short illumination time, a more plausible reaction mechanism of $^\bullet CO_2^-$ generation from bicarbonate reduction is proposed in Scheme 1, involving simultaneous transfer of electrons and protons.

SCHEME 1

In Figure 6 we report the intensity of the [pbn-CO_2^-]$^\bullet$ adduct recorded at a fixed field position after 3 min illumination of some commercial TiO_2 samples in a HCO_3^- solution at a neutral pH. For a comparative analysis one must consider that surface area is an important parameter and since it is significantly different for the examined samples (50 to 320 m^2/g), all signal intensities have been normalized to the known surface areas. It is the significantly higher amount of $^\bullet CO_2^-$ radicals produced on P25 that meets the eye and results are seemingly not directly correlated to areas.

FIGURE 6

An analogous comparative analysis of $OH^{\bullet}$ production measured by coumarin hydroxylation, on different TiO_2 samples, showed that the activity of PC 500 is about one half that of PC50 despite the area of the former is 6 times higher. This is less surprising than might seem at first and, in fact, concerning surface reactions, it has been previously remarked that there can be real or apparent effects depending on the factors at the origin of the effect itself. If surface structure and chemical composition (electronic factors) prevail, catalysis is "real". Alternatively, if the origin of the effect is simply related to surface area one can speak of "apparent" catalysis, since it vanishes as surface area effects are accounted for.[33]

The lack of correlation between activity and surface area for reduction and oxidation processes calls for an explanation that relies on the contribution of different surface characteristics including, for example, defects and the surface density of OH groups. [34, 35]

In relation to the P25 data in Figure 6, we limit ourselves to remarking that according to the literature,[36, 37] a likely explanation is the anatase/rutile mixed structure of this catalyst that helps charge separation thus reducing recombination. It has been previously remarked that P25 often turns out to be a more active catalyst than others having a higher specific surface area,[38] stressing the importance of a good charge carrier separation.

Apart from P25, the other three samples examined are made of pure anatase and arguably the higher activity of TiO_2-PC105 has still another explanation. We think it is presumably connected with an enhanced adsorption of bicarbonate anions on a comparatively high number of Lewis acid sites that characterizes this particular sample.[39]

During the course of the above described experiments, we have never detected $H^{\bullet}$ radicals and neither were they observed in previous literature,[20] but we cannot *a priori* exclude that HCO_2^- is the result of an indirect, fast reduction of HCO_3^- by $H^{\bullet}$, if reduction of water preferentially occurs instead

of reaction (3). The pH dependent thermodynamic standard potentials involving species that are relevant to this work (HCO_3^-, H_2CO_3, HCO_2^-) are:[40]

$E_o = -0.078 - 0.0591$ pH (HCO_2^-/ HCO_3^-) (11)

$E_o = -0.267 - 0.0295$ pH (HCO_2^-/ H_2CO_3) (12)

$E_o = -0.156 - 0.0591$ pH (HCO_2H/ H_2CO_3) (13)

$E_o = 0.0 - 0.0591$ pH (H_2/H_2O) (14)

At pH 7, potentials for reactions (11-13) are comparable and more positive than E_{fb} (-0.57 V, vs NHE), but slightly more negative than that of H_2O reduction, i.e., -0.42 V (NHE), which is then expected to be favored. It is important to point out, however, that oxides do not take the reversible potential of the H_2 reaction because, unlike the case of metals, H_2 is not dissociatively adsorbed.[41] More generally, standard conditions do not quite represent real ones.

Metal-modified TiO_2

In the previous paragraph we concluded that we cannot prove or disprove reduction of HCO_3^- by $H^\bullet$. At least in short timescale experiments, a mechanism involving these radicals may appear unconvincing due to the known kinetic limitations of H_2O reduction. It is shown in this paragraph that for TiO_2 modified with some noble metals nanoparticles, the role of $H^\bullet$ can become clearer.

In the case of Pd(1%)-TiO_2 the role of hydrogen in the reduction of HCO_3^- to $^\bullet CO_2^-$ is strikingly evident from the data of Fig. 7. The intensity of the [pbn-CO_2^-]$^\bullet$ signal increases and reaches a plateau as a function of illumination time; on switching off the light at this point, one observes that the signal grows again. This effect can be interpreted as a manifestation of $H^\bullet$ participation in the reduction process (Scheme 2) that, as proposed earlier,[15] is promoted by the ability of palladium to

store hydrogen by forming stable metal-hydride bonds. This property is in fact the basis of an interesting method of storage and generation of hydrogen by the bicarbonate/formate reaction.[42] Analogous experiments with Rh(1%)-TiO_2 showed a comparable activity of $^{\bullet}CO_2^-$ formation under illumination, but the dark growth seen in Fig. 7 was absent. Both Pd and Rh can work as sink of electrons but the important difference lies in the reported ability of the former is to form more stable hydrides.

Scheme 2

FIGURE 7

The last composite catalyst we examined was Ru(1%)-TiO_2, which shows still another behavior. The EPR spectrum is rather complex (ESI Fig. 3) as it reveals not only trapped $OH^{\bullet}$ and $^{\bullet}CO_2^-$ radicals but also a $[pbn\text{-}CO_3^-]^{\bullet}$ adduct (Eq. 5) whose signal intensity grows with illumination time even at pH 7. In this case, a likely explanation [43] is that initially Ru^0 sites are oxidized by holes to Ru^{n+}, i.e., hydrated species of the type $RuO(OH)_x$, which feature very good oxidizing power. These results demonstrate that the kind of metal chosen for surface modification cannot be arbitrary.

Experimental

Materials and methods

Several commercial TiO_2 samples were used in this study. Metal nanoparticles modifications of TiO_2-P25 were obtained following the procedure described by Goren et al. [14].

Apparatus

EPR spin trapping experiments were performed with a Bruker ER 200MRD spectrometer equipped with a TE 201 resonator, at a microwave frequency of 9.4 GHz. Irradiations were carried out directly inside the EPR cavity with a Hanau Q-400 medium-pressure Hg lamp using a cut off filter ($\lambda > 360$ nm). The settings for the EPR spectrometer were as follows: center field, 3460 G; sweep width, 50 G; microwave frequency 9.4 GHz; modulation frequency 100 kHz; power, 6.3 mW; sweep time 41.94 s. The same flat quartz EPR cell was used for all measurements in order to minimize experimental errors.

Fluorescence spectra were recorded with a Jobin Yvon Spex Fluoromax II spectrofluorimeter equipped with a Hamamatsu R3896 photomultiplier. Both emission and excitation slits were set at 5.0 nm during the measurements. Irradiations that precede fluorescence measurements were performed with a Hg medium pressure lamp analogous to that described above. All the experiments were carried out in O_2-free suspensions at atmospheric pressure and at room temperature.

EPR spin trapping experiments

Concentrated suspensions of the photocatalyst (20 g/L) in aqueous solutions containing α-phenyl N-*tert*-butyl nitrone (pbn, 0.1 M) were prepared both in the absence and in the presence of $NaHCO_3$ (0.01 M). In this last case, the initial pH of the solutions was 8.8. The suspensions were first deaerated with argon and pH was lowered by bubbling CO_2 for a time that depended on the requested pH value (7.5 ÷ 4), as established by preliminary tests. Subsequently, the deoxygenated suspensions in a closed vessel were quickly transferred inside the flat EPR quartz cell inside a dry-box under inert atmosphere. In the experimental pH interval 7.5 ÷ 4, HCO_3^- is in equilibrium with dissolved CO_2 and we have checked that CO_2 loss into the gas phase during the transfer is negligible on the basis of pH measurements as well as using a CO_2 gas sensor (Thermo Scientific).

EPR spin trapping spectra were recorded as a function of irradiation time. No signals were obtained in the dark before irradiation. The amount of employed spin trap is in large excess and it has been optimized on the basis of the dependence of the signal intensity from spin trap concentration.

Fluorescence measurements

The samples were constituted by suspensions of the photocatalyst (about 3.5 mg/mL) in aqueous solutions containing coumarin (1.15×10^{-4} M) and when requested $NaHCO_3$ (0.01 M) at pH 7.2-7.5.

A suspension (3 mL), at the desired pH value and deaerated as described above, was irradiated under magnetic stirring for 15 minutes ($\lambda > 360$ nm) in a Pyrex reactor (total volume 10 mL) provided with a 1 cm wide flat window. After irradiation the suspension was centrifuged and the fluorescence spectrum (λ_{exc}= 332 nm) of 7-hydroxycoumarin, eventually formed, was recorded (λ_{emiss}= 455 nm) using a standard fluorimetric quarz cell.

In order to verify the effect of possible pH changes during irradiation, parallel control experiments were carried out in the presence of diluted Na_2HPO_4/NaH_2PO_4 buffer. No difference was noted in the indicating that pH changes are negligible and that possible phosphate adsorption on TiO_2 does not affect formation of 7-hydroxycoumarin.

Conclusions

An EPR spin trapping investigation shows that parallel reactions take place in illuminated suspensions of TiO_2 in aqueous carbonate solutions (pH ≈ 7) which involve the formation of $OH^{\bullet}$ radicals from photo-oxidation of water and carbon-oxygen radical species resulting from the redox reactions of bicarbonate (HCO_3^-). The salient results are:

- The efficiency of formation of $OH^{\bullet}$ radicals is proportional to the concentration of bicarbonate and depends on pH, as confirmed by an independent method using coumarin hydroxylation. In a weakly alkaline medium, photo-oxidation of HCO_3^- to $^{\bullet}CO_3^-$ becomes evident. This process interferes with the oxidation of water.
- The EPR measurements show the formation of $^{\bullet}CO_2^-$ radicals in suspensions containing bicarbonate at pH 5.5÷7.5, confirming its reduction to formate as the initial stage. These radicals are not seen at pH 4 where dissolved CO_2 is the main species indicating that HCO_3^- in solution is the reducible species.
- The use of samples of different commercial origin shows that the efficiency of ($^{\bullet}CO_2^-$) formation is not directly correlated with the surface area of the photocatalysts. Allowing for this important parameter reveals that an explanation of the results must rely on the contribution of other factors related to the surface structure that condition adsorption phenomena and recombination of photogenerated charges.
- The effect of surface modification by noble metals on the amount of ($^{\bullet}CO_2^-$) detected depends on the nature of the metal. The radical is formed with high efficiency on illuminated Pd-TiO_2 and Rh-TiO_2; in the first case, the intensity of the EPR signal continues to grow after light is switched off strongly suggesting participation of hydrogen in the reduction of bicarbonate. Among the metal modified catalysts Ru-TiO_2 features the peculiarity of favouring HCO_3^- oxidation. This is likely due to formation of oxidised surface species of the type $RuO(OH)_x$ which, according to published literature, feature a very good oxidizing power. The results demonstrate that the kind of metal chosen for surface modification cannot be arbitrary.

In general, identification of radical intermediates of oxidation and reduction reactions can provide useful mechanistic information that may be used in the development of photocatalytic systems for the reduction of CO_2 also stored in the form of carbonates.

Acknowledgements

We kindly acknowledge MIUR PON01_02257 for financial support.

References

1 M. Aresta in *"Carbon Dioxide as Chemical Feedstock"* WILEY-VCH Verlag, Weinheim, 2010.

2. G. Centi and S. Perathoner, *Catal. Today*, 2009, **148**, 191.

3. E. Benson, P. Kubiak, A. Clifford, J. Sathrum and J. M. Smieja, *Chem. Soc. Rev.*, 2009, **38**, 89.

4. E. V. Kondratenko, G. Mul, J. Baltrusaitis, G. O. Larrazabal and J. Perez-Ramirez, *Energy Environ. Sci.*, 2013, **6**, 3112.

5. S. N. Habisreutinger, L. Schmidt-Mende and J. K. Stolarczyk, *Angew. Chem. Int. Ed.*, 2013, **52**, 2.

6. Y. Hori in *Modern Aspects of Electrochemistry*, C. Vayenas et al. (eds), Springer, New York, 2008, Vol. **42**, 89-189.

7. P. Indrakanti, J. D. Kubickib and H. H. Schobert, *Energy Environ. Sci.*, 2009, **2**, 745.

8**.** H. He, P. Zapol and L. A. Curtiss, *J. Phys. Chem. C*, 2010, **114**, 21474.

9. G. Centi, S. Perathoner, G. Winè and M. Gangeri, *Green Chem.*, 2007, **9**, 671.

10. Y. Izumi, *Coord. Chem. Rev.*, 2013, **257**, 171.

11. G. Mele, C. Annese, A. De Riccardis, C. Fusco, L. Palmisano, G. Vasapollo and L. D'Accolti, *Appl. Catal. A - General*, 2014, **481**, 169.

12. K**.** Li, A**.** D. Handoko, M**.** Khraisheh and J**.** Tang, *Nanoscale***,** 2014, **6,** 9767.

13 .C. J. Stalder, S. Chao and M. S. Wrighton, *J. Am. Chem. Soc.*,1984, **106**, 3673.

14. H.S. Freund and M.W. Roberts, Surf. Sci. Reports, 1996, 25, 225

15. Z. Goren, I. Willner, A. J. Nelson and A. J. Frank, *J. Phys. Chem*, 1990, **94**, 3784.

16. C. C. Yang, J. Vernimmen, V. Meynen, P. Cool and G. Mul, *J. Catal.*, 2011, **284**, 1.

17. R. Kortlever, K. H. Tan, Y. Kwon and M. T. M. Koper, *J. Solid State Electrochem.*, 2013, **17**, 1843.
18. X. G. Meng, S. X. Ouyang, T. Kako, P. Li, Q. Yu, T. Wang and J. H. Ye, *Chem. Commun.*, 2014, **50**, 11517.
19. N. Sreekanth and K. L. Phani, *Chem.Commun.*, 2014, **50**, 11143.
20. N. M. Dimitrijevic, B. K. Vijayan, O. G. Poluektov, T. Rajh, K. A. Gray, H. He and P. Zapol, *J. Am. Chem. Soc.*, 2011, **133**, 3964.
21. H. Fu, L. Zhang, S. Zhang, Y. Zhu and J. Zhao, *J. Phys. Chem. B*, 2006, **110**, 3061.
22. A. Di Paola, M. Bellardita, L. Palmisano, Z. Barbierikova and V. Brezova, *J. Photochem. Photobiol. A: Chem.*, 2014, **273**, 59.
23. A. Molinari, R. Argazzi and A. Maldotti, *J. Mol. Catal. A: Chem.*, 2013, **372**, 23.
24. A. Molinari, G. Magnacca, G. Papazzoni and A. Maldotti, *Appl. Catal. B Environ.*, 2013, **138-139**, 446.
25. A. Molinari, A. Maldotti and R. Amadelli, *Chem. Eur. J.*, 2014, **20**, 7759.
26. G. R. Buettner, *Free Rad. Biol. & Medicine*, 1987, **3**, 259.
27. F. A. Villamena, E. J. Locigno, A. Rockenbauer, C. M. Hadad and J. L. Zweier, *J. Phys. Chem. A*, 2006, **110**, 13253.
28. R. Amadelli, A. Maldotti, C. Bartocci and V. Carassiti, *J. Phys. Chem.*, 1989, **93**, 6448.
29. B. Aurian-Blajeni, M. Halmann and J. Manassen, *Photochem. Photobiol.*, 1982, **35**, 157.
30. K. Sayama and H. Arakawa, *J. Chem. Soc., Faraday Trans.*, 1997, **93**, 1647.
31. H. Czili and A. Horvath, *Appl. Catal. B: Environ.*, 2008, **81**, 295**.**
32. U. Černigoj, U. Lavrenčič Štangar, P. Trebšea, M. Sarakhab, *J. Photochem. Photobiol. A: Chem.*, 2009, **201**, 142.
33. E. Guerrini and S. Trasatti, *Russ. J. Electrochem.*, 2006, **42**, 1017.
34. K. Kobayakawa, Y. Nakazawa, M. Ikeda and A. Fujishima, *Ber. Bunsenges. Phys. Chem.*, 1990, **94,** 1439.
35. A. Di Paola, M. Bellardita, L. Palmisano, Z. Barbieriková, V. Brezová, *J. Photochem. Photobiol. A: Chem.*, 2014, **273**, 59.]
36. D. C. Hurum, A. G. Agrios, K. A. Gray, T. Rajh and M. C. Thurnauer, *J. Phys. Chem. B***,** 2003, **107**, 4545.
37. J. T. Carneiro, T. J. Savenije, J. A. Moulijn, and G. Mul, *J. Phys. Chem. C*, 2011, **115**, 2211.

38. D. D'Elia, C. Beauger, J. F. Hochepied, A. Rigacci, M. H. Berger, N. Keller, V. Keller-Spitzer, Y. Suzuki, J. C. Valmalette, M. Benabdesselam and P. Achard, *J. Hydrogen Energy*, 2011, **36**, 14360.

39. R. Amadelli et al. unpublished work.

40. M. Pourbaix, "Atlas of electrochemical equilibria in aqueous solutions", National Association of Corrosion Engineers, Houston, 1974.

41. S. Trasatti in *Interfacial Electrochemistry: Theory, Experiment, and Applications,* A. Wieckowski (Ed.), Marcel Dekker, Inc. New York, 1999, pp.769-792.

42. H. Kramer, M. Levy and A. Warshawsky, *Int. J. Hydrogen Energy*, 1995, **20**, 229.

43. P. Panagiotopoulou, D. I. Kondarides and X. E. Verykios, *J. Phys. Chem. C***,** 2011, **115**, 1220.

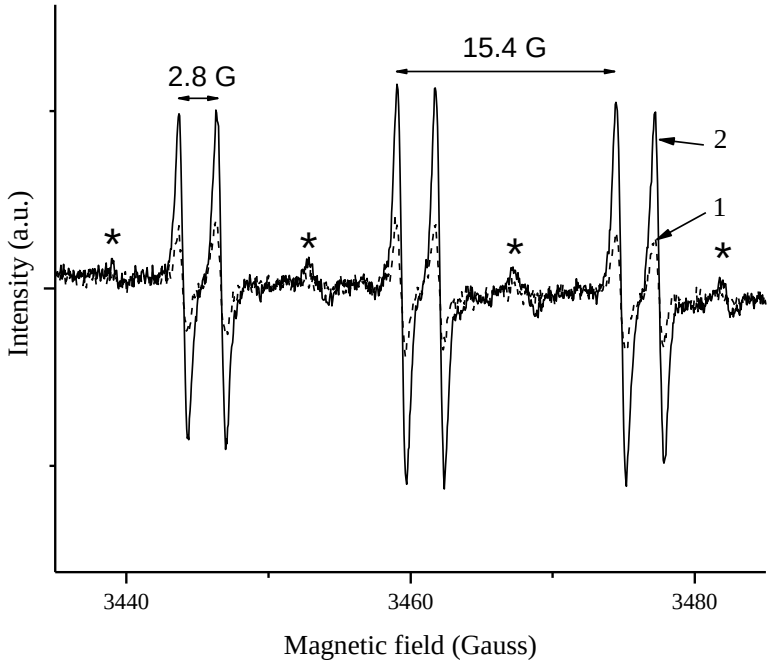

Figure 1. EPR spectra obtained upon irradiation ($\lambda > 360$ nm) of deaerated aqueous suspensions of TiO_2- P25 containing pbn (0.1 M) at pH 7.2 ÷ 7.5 in the absence (curve 1) and in the presence of $NaHCO_3$ (0,01 M)/CO_2 (curve 2).

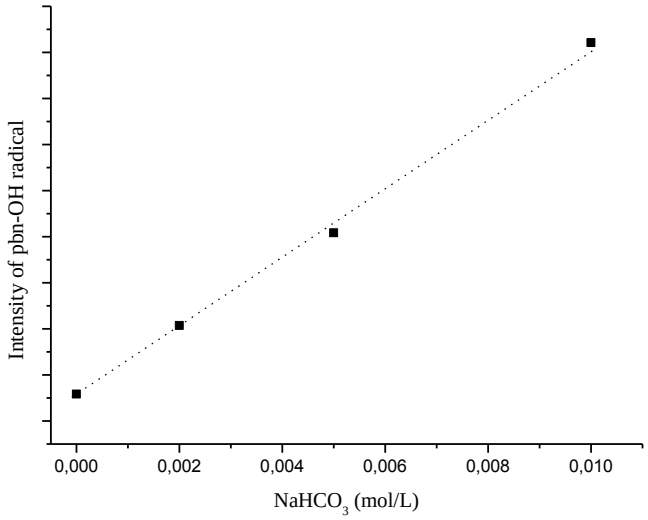

Figure 2. Intensity of [pbn-OH]· adduct as a function of $NaHCO_3$ concentration obtained upon irradiation (λ > 360 nm) of TiO_2-P25 deaerated aqueous suspensions containing pbn (0.1 M). pH is maintained in the range 6.8-7.5 by bubbling CO_2.

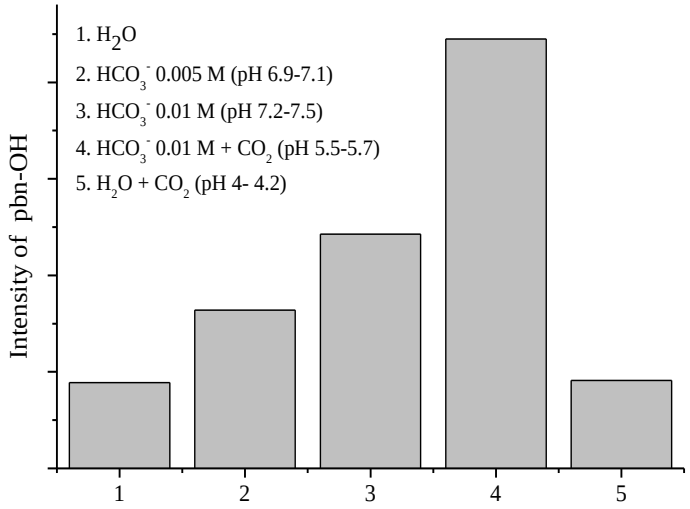

Figure 3. Comparison of the intensities of [pbn-OH]· adduct obtained upon irradiation of TiO_2-P25 deaerated aqueous suspensions containing pbn (0.1M) with different concentrations of $NaHCO_3$. Columns 4 and 5 are relative to samples deaerated with CO_2.

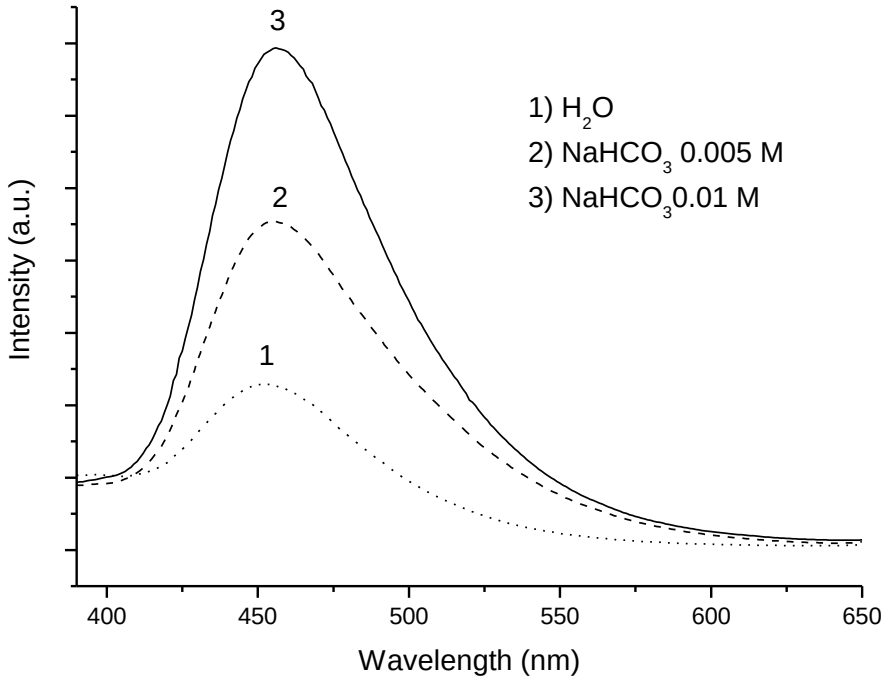

Figure 4. Emission intensity of 7-HC measured at 455 nm obtained on illumination (15 min) of deaerated aqueous suspensions of TiO_2-P25 containing coumarin (1×10^{-4} M).

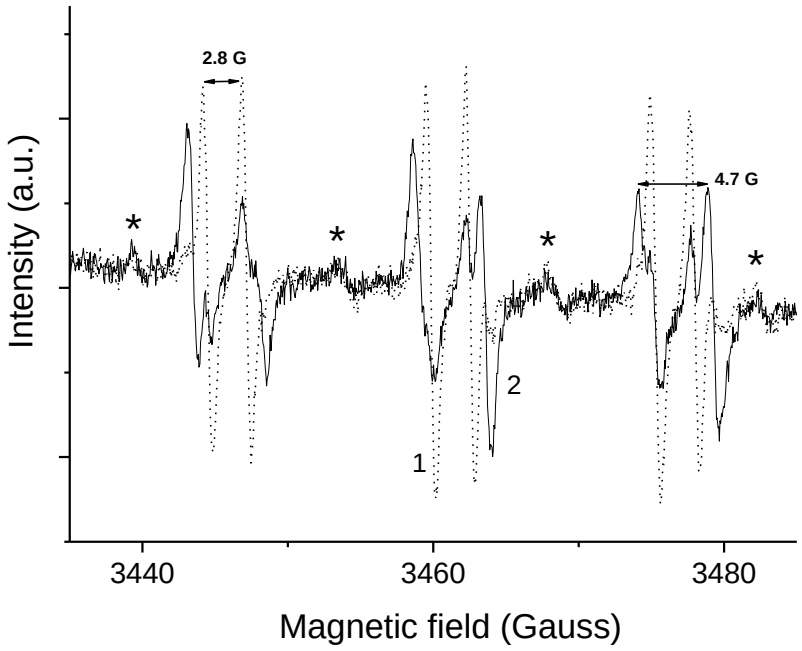

Figure 5. EPR spectra obtained on illumination for 30 s (curve 1) and 3 min (curve 2) of deaerated TiO_2-P25 suspensions in an aqueous solution of $NaHCO_3$ 0,01 M and pbn (0.1 M) at pH 7.2 ÷ 7.5.

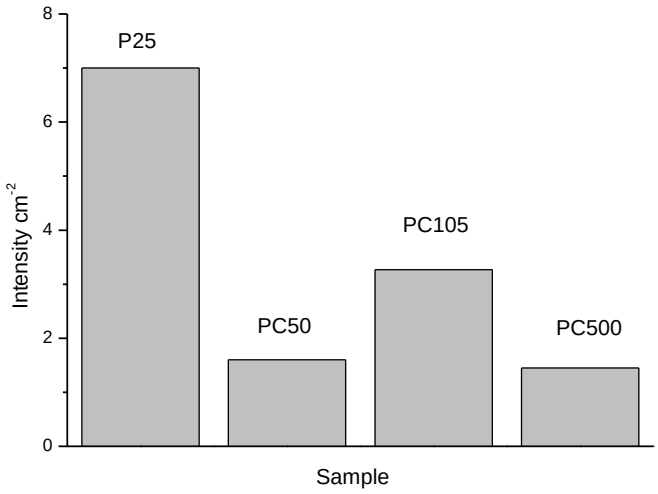

Figure 6. Intensity of the [pbn-CO_2^-]· adduct normalized by the area of the sample obtained on illumination (3 min) of different commercial TiO_2 powders dispersed in deaerated aqueous solutions containing $NaHCO_3$ (0.01M) and pbn (0.1 M). pH 7.2 ÷ 7.5.

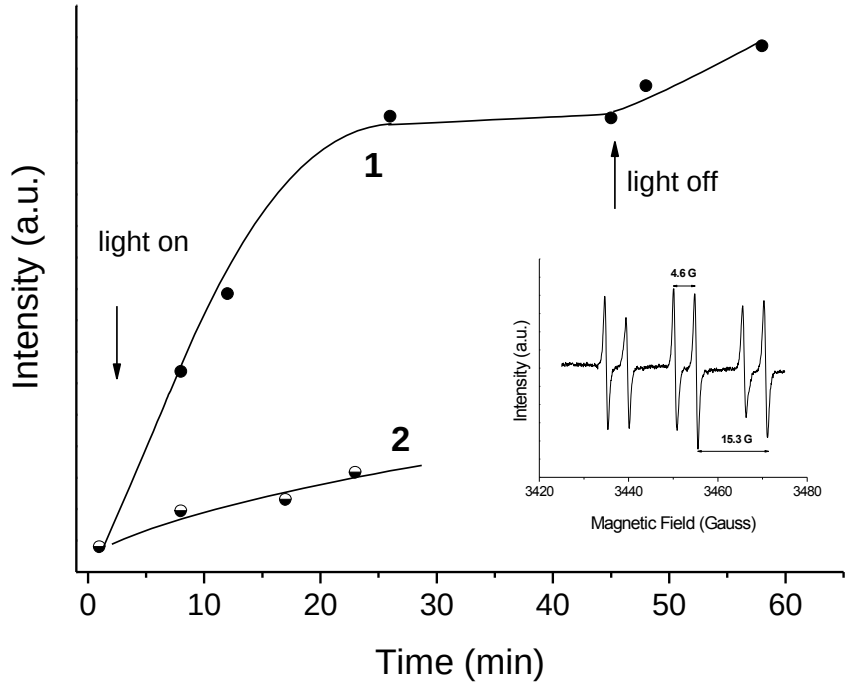

Figure 7. Intensity of the [pbn-CO_2^-]· as a function of illumination time for Pd(1%)-TiO_2 (curve 1) and TiO_2-P25 (curve 2) suspensions in an aqueous solution of $NaHCO_3$ 0,01 M and pbn (0.1 M) at pH 7.2 ÷ 7.5. The inset shows the signal of the EPR signal at t = 10 min.